An Efficient Numerical Method for Analyzing Photonic Crystal Slab Waveguides

Lijun Yuan and Ya Yan Lu

Department of Mathematics, City University of Hong Kong, Hong Kong

Computing the eigenmodes of a photonic crystal (PhC) slab waveguide is computationally expensive, since it leads to eigenvalue problems in three-dimensional domains which are large compared with the wavelength. In this paper, a procedure is developed to reduce the eigenvalue problem for PhC slab waveguides to a nonlinear problem defined on a small surface in the waveguide core. The reduction process is efficiently performed based on the so-called Dirichlet-to-Neumann maps of the unit cells. The nonlinear eigenvalue problem can be efficiently solved by standard root-finding methods, such as the secant method.

OCIS codes: 130.5296,050.5298,000.4430

1. Introduction

In recent years, many compact photonic components and devices have been designed and fabricated using photonic crystals (PhCs) for potential applications in integrated optical circuits [1]. Most of these structures rely on the bandgap effect and consist of defects in an otherwise perfectly periodic PhC. Although a three-dimensional (3D) PhC has better light confinement capability, a PhC slab which has a two-dimensional (2D) periodic pattern in a layered medium is much easier to fabricate and widely used. A typical PhC slab consists of a triangular lattice of air holes in a high-index dielectric slab surrounded by lower-index media. In a PhC slab, a waveguide can be introduced by filling a row of air holes [2–6]

To design and optimize PhC slab waveguides, efficient numerical methods are needed for computing the waveguide modes. The 3D finite-difference time-domain (FDTD) method has been used to analyze PhC slab waveguides [4, 5], but it requires long computing time. This is especially true for structures with large index-contrast, where a very small grid size is needed to resolve the interfaces. In the frequency domain, the standard formulation leads to an eigenvalue problem in a 3D region S which covers one period along the waveguide axis and is unbounded in the two transverse directions. To find the dispersion relations of the waveguide modes, the eigenvalue problem must be solved for various values of the

propagation constant (the Bloch wavenumber). Standard numerical methods, such as the plane wave expansion method [6] and the finite element method [7], can be used to solve this eigenvalue problem. For the finite element method, it is necessary to truncate the unbounded directions of S and discretize the truncated domain. For the plane wave expansion method, the unbounded directions of S may be truncated with periodic boundary conditions, and then the electromagnetic fields are expanded into Fourier series. All these methods give rise to matrix eigenvalue problems involving very large matrices. To find accurate solutions for the waveguide modes by these methods, prohibitive computer resources (including both CPU time and memory) are usually needed. In an alternative frequency-domain formulation, a PhC slab waveguide can be analyzed for given frequencies with eigenvalues related to the Bloch wavenumber. This can be achieved by using the scattering matrix for one period of the PhC slab waveguide [8]. The eigenvalue problem is linear even for dispersive media, and the involved matrices are smaller but non-sparse. Unfortunately, this approach is still quite expensive, since the scattering matrix is not easy to calculate and the eigenvalue problem with dense matrices is not easy to solve. Furthermore, an even smaller but nonlinear eigenvalue problem was obtained using a lateral scattering matrix formalism [9], but these scattering matrices are calculated based on a lateral staircase approximation of the structure which limits the accuracy.

Recently, some efficient numerical methods based on the Dirichlet-to-Neumann (DtN) maps of the unit cells have been developed to analyze waveguides in ideal 2D PhCs which have an invariant direction [10, 11]. The DtN map of a unit cell is an operator that maps the wave fields to their normal derivatives on the cell boundary, and it can be approximated by a small matrix. Similar to the methods based on the scattering matrices [8, 9], the DtN map method solves eigenvalue problems for fixed frequencies, and it gives either a linear eigenvalue problem with relatively small matrices [10] or a nonlinear eigenvalue problem with even smaller matrices [11]. Notice that the DtN map method was first used to calculate transmission and reflection spectra for PhCs which are finite in one periodic direction [12]. In a previous work [13], we extended the method to compute transmission and reflection spectra of PhC slabs with finite number of air-hole arrays. The key step is to construct DtN maps for 3D unit cells of PhC slabs. Such a DtN map involves two field components and is constructed using expansions in vertical slab modes and horizontal cylindrical waves. In this paper, we develop an efficient method for analyzing PhC slab waveguides based on the DtN maps constructed in [13]. Our method extends the nonlinear eigenvalue approach described in [11] to the 3D problem for PhC slab waveguides.

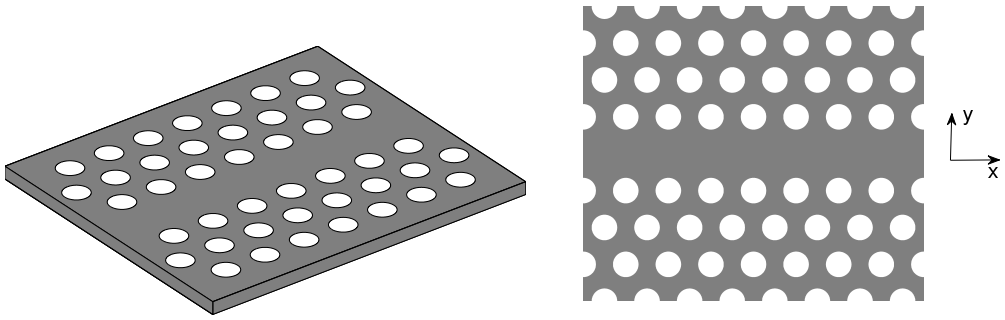

Fig. 1. A PhC slab waveguide formed by filling one row of air holes in a PhC slab: (a) the 3D view; (b) the top view.

2. Linear eigenvalue problems

In a PhC slab consisting of air holes on a triangular lattice, a PhC slab waveguide can be formed by filling a row of air holes as shown in Fig. 1. Let $\{x, y, z\}$ be a Cartesian coordinate system, we assume that the slab is perpendicular to the z axis, the original PhC is periodic in x with period L (the lattice constant) and the filled row is in the x-direction, then the PhC slab waveguide is periodic in x. The structure can be described by its dielectric function $\varepsilon(x, y, z)$ and relative magnetic permeability $\mu(x, y, z)$, where ε and μ are periodic in x with period L.

Our starting point is the frequency-domain Maxwell's equations:

$$\nabla \times \boldsymbol{E} = ik_0\mu\boldsymbol{H}, \quad \nabla \times \boldsymbol{H} = -ik_0\varepsilon\boldsymbol{E}, \tag{1}$$

where $\boldsymbol{E}$ is the electric field, $\boldsymbol{H}$ is the magnetic field multiplied by the free space impedance, ω is the angular frequency and k_0 is the free space wavenumber. The time dependence is assumed to be $e^{-i\omega t}$. For a PhC slab waveguide, we look for Bloch modes given as

$$\begin{bmatrix} \boldsymbol{E} \\ \boldsymbol{H} \end{bmatrix} = \begin{bmatrix} \boldsymbol{\Phi} \\ \boldsymbol{\Psi} \end{bmatrix} e^{i\beta x}, \tag{2}$$

where β is the Bloch wavenumber (i.e. the propagation constant), $\boldsymbol{\Phi}$ and $\boldsymbol{\Psi}$ are periodic in x with period L. A Bloch mode is a guided mode if β is real, and $\boldsymbol{\Phi}$ and $\boldsymbol{\Psi}$ tends to zero as $|y|$ or $|z|$ tends to infinity. Clearly, a Bloch mode satisfies the following quasi-periodic condition:

$$\begin{bmatrix} \boldsymbol{E}(x+L, y, z) \\ \boldsymbol{H}(x+L, y, z) \end{bmatrix} = \rho \begin{bmatrix} \boldsymbol{E}(x, y, z) \\ \boldsymbol{H}(x, y, z) \end{bmatrix} \tag{3}$$

where $\rho = e^{i\beta L}$.

Standard numerical methods solve Eq. (1) on one period of the waveguide S as an eigenvalue problem, where the eigenvalue is ω^2 (or k_0^2) and β is a real parameter. Notice that one period of the waveguide is a 3D volume given by

$$S = \{(x, y, z) : 0 < x < L, -\infty < y < \infty, -\infty < z < \infty\}. \tag{4}$$

This is a linear eigenvalue problem for non-dispersive media, but it becomes nonlinear if the medium is dispersive. Alternatively, we can fix ω and solve for β. Based on Eq. (2), it is simple to derive equations for $\mathbf{\Phi}$ and $\mathbf{\Psi}$, and these equations give rise to an eigenvalue problem on S where β is the eigenvalue. This is a linear eigenvalue problem even for dispersive media. Numerical methods based on both approaches must discretize the domain S or expand functions defined on S in a suitable basis, and consequently, the resulting matrix eigenvalue problems involve very large matrices and are difficult to solve.

For a fixed ω, it is possible to formulate eigenvalue problems for PhC slab waveguides on a surface, for example, the plane at $x = 0$. The scattering operator approach assumes that the electromagnetic fields at $x = 0$ and $x = L$ can be decomposed as forward (increasing x) and backward (decreasing x) components. Using the z components $\boldsymbol{w} = [E_z, H_z]^T$ and denoting the directional components by superscripts $\pm$, the scattering operator $\mathcal{S}$ satisfies

$$\mathcal{S} \begin{bmatrix} \boldsymbol{w}^+|_{x=0} \\ \boldsymbol{w}^-|_{x=L} \end{bmatrix} = \begin{bmatrix} \mathcal{S}_{11} & \mathcal{S}_{12} \\ \mathcal{S}_{21} & \mathcal{S}_{22} \end{bmatrix} \begin{bmatrix} \boldsymbol{w}^+|_{x=0} \\ \boldsymbol{w}^-|_{x=L} \end{bmatrix} = \begin{bmatrix} \boldsymbol{w}^-|_{x=0} \\ \boldsymbol{w}^+|_{x=L} \end{bmatrix}. \tag{5}$$

Meanwhile, the quasi-periodic condition (3) leads to $\boldsymbol{w}^{\pm}|_{x=L} = \rho \boldsymbol{w}^{\pm}|_{x=0}$. Eliminating $\boldsymbol{w}^{\pm}|_{x=L}$ in (5), we obtain the following generalized eigenvalue problem for ρ:

$$\begin{bmatrix} \mathcal{S}_{11} & -\mathcal{I} \\ \mathcal{S}_{21} & 0 \end{bmatrix} \begin{bmatrix} \boldsymbol{w}^+|_{x=0} \\ \boldsymbol{w}^-|_{x=0} \end{bmatrix} = \rho \begin{bmatrix} 0 & -\mathcal{S}_{12} \\ \mathcal{I} & -\mathcal{S}_{22} \end{bmatrix} \begin{bmatrix} \boldsymbol{w}^+|_{x=0} \\ \boldsymbol{w}^-|_{x=0} \end{bmatrix}. \tag{6}$$

Matrix approximations to the above can be obtained by expanding $\boldsymbol{w}^{\pm}|_{x=0}$ in plane waves [8]. Another formulation is based on the DtN operator $\mathcal{G}$ which satisfies

$$\mathcal{G} \begin{bmatrix} \boldsymbol{w}|_{x=0} \\ \boldsymbol{w}|_{x=L} \end{bmatrix} = \begin{bmatrix} \mathcal{G}_{11} & \mathcal{G}_{12} \\ \mathcal{G}_{21} & \mathcal{G}_{22} \end{bmatrix} \begin{bmatrix} \boldsymbol{w}|_{x=0} \\ \boldsymbol{w}|_{x=L} \end{bmatrix} = \begin{bmatrix} \partial_x \boldsymbol{w}|_{x=0} \\ \partial_x \boldsymbol{w}|_{x=L} \end{bmatrix}. \tag{7}$$

The quasi-periodic condition (3) implies

$$\boldsymbol{w}|_{x=L} = \rho \boldsymbol{w}|_{x=0}, \quad \partial_x \boldsymbol{w}|_{x=L} = \rho \partial_x \boldsymbol{w}|_{x=0}. \tag{8}$$

Therefore, we can eliminate $\boldsymbol{w}|_{x=L}$ and $\partial_x \boldsymbol{w}|_{x=L}$ and obtain an eigenvalue problem for ρ:

$$\begin{bmatrix} \mathcal{G}_{11} & -\mathcal{I} \\ \mathcal{G}_{21} & 0 \end{bmatrix} \begin{bmatrix} \boldsymbol{w}|_{x=0} \\ \partial_x \boldsymbol{w}|_{x=0} \end{bmatrix} = \rho \begin{bmatrix} 0 & -\mathcal{G}_{12} \\ \mathcal{I} & -\mathcal{G}_{22} \end{bmatrix} \begin{bmatrix} \boldsymbol{w}|_{x=0} \\ \partial_x \boldsymbol{w}|_{x=0} \end{bmatrix}. \tag{9}$$

Still other approaches exist. For example, the impedance operator that maps $[E_y, E_z]^T$ to $[H_y, H_z]^T$ on the two planes at $x = 0$ and $x = L$, can also be used to formulate an eigenvalue problem for ρ. The eigenvalue problems (6) and (9) are linear even for dispersive media. Since they are defined on a surface (instead of a volume S), they give rise to smaller matrices, but $\mathcal{S}$ and $\mathcal{G}$ are not easy to obtain and they are usually approximated by dense matrices. Therefore, it is still very expensive to calculate PhC waveguide modes based on these formulations.

3. Nonlinear formulation

In this section, we formulate a nonlinear eigenvalue problem for computing PhC slab waveguide modes. The original domain S for one period of the waveguide is unbounded in both y and z. Due to the bandgap effect, the electromagnetic fields decay to zero as $y \to \pm\infty$, therefore, we can truncate S to a domain S_m containing $2m+1$ unit cells as shown in Fig. 2 (for $m = 4$). These unit cells (Ω_j for $1 \le j \le 2m+1$) are bounded by two planes at $x = 0$

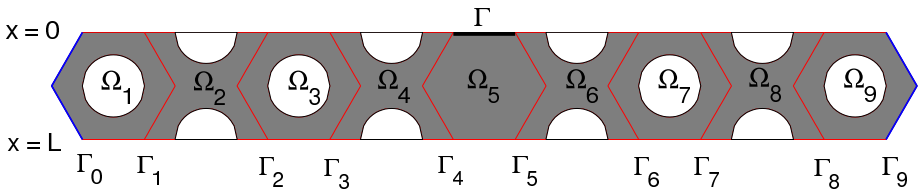

Fig. 2. The top view of the truncated domain S_m ($m = 4$) for one period of a PhC slab waveguide. Also shown are the unit cells Ω_j, the lateral surfaces Γ_j and the special surface Γ.

and $x = L$, separated by lateral surfaces Γ_0, Γ_1, ..., Γ_{2m+1}, and are still unbounded in the z directions. We denote the cross section of Ω_j by Ω_j^0, and it is a domain in the xy plane. There are three different types of unit cells, namely, the central (or defect) unit cell (Ω_5 in Fig. 2) corresponding to the waveguide core, the regular unit cells (Ω_1, Ω_3, Ω_7, Ω_9 in Fig. 2) containing entire air holes and the concave unit cells (Ω_2, Ω_4, Ω_6, Ω_8 in Fig. 2) containing half air holes. The cross sections of the central and regular unit cells are regular hexagons, while the concave unit cells have concave hexagon cross sections. On the left and right surfaces Γ_0 and Γ_{2m+1}, we assume $\boldsymbol{w} = [E_z, H_z]^T$ is zero.

The boundary of the central unit cell (Ω_5 in Fig. 2) contains a flat segment Γ which is a strip in the plane at $x = 0$. We reduce the waveguide eigenvalue problem to

$$\mathcal{B}(\omega, \beta)\, \boldsymbol{w}|_\Gamma = 0, \tag{10}$$

where $\mathcal{B}$ is an operator that depends on the frequency ω and the Bloch wavenumber β. This

is a nonlinear eigenvalue problem. It can be solved by searching ω or β from

$$\lambda_1(\mathcal{B}) = 0, \tag{11}$$

where λ_1 is the eigenvalue of $\mathcal{B}$ with the smallest magnitude. Eq. (11) can be solved by standard root-finding methods, such as the secant method.

Clearly, it is essential to have an efficient method to calculate the operator $\mathcal{B}$ for given ω and β. Four steps are needed to achieve this. The first step is to calculate the DtN maps of the central and the regular unit cells. For a unit cell Ω_j with a hexagon cross section Ω_j^0, the DtN map Λ_j is an operator satisfying

$$\Lambda_j \boldsymbol{w} = \partial_{\boldsymbol{\nu}} \boldsymbol{w} \quad \text{on} \quad \partial\Omega_j, \tag{12}$$

where $\partial\Omega_j$ denotes the lateral boundary of Ω_j, $\boldsymbol{\nu}$ is a unit normal vector of $\partial\Omega_j$ and $\partial_{\boldsymbol{\nu}}\boldsymbol{w}$ is the normal derivative of $\boldsymbol{w}$. A detailed construction for Λ_j can be found in our earlier work [13]. The main idea is to write down the general solution of $\boldsymbol{w}$ in Ω_j and use it to construct a matrix approximation for Λ_j. The general solution in Ω_j (outside the air hole) can be written down as a double-sum expansion involving the vertical slab modes and horizontal cylindrical waves. The slab without the air holes is a waveguide with a one-dimensional refractive index profile, and its eigenmodes are referred to as the vertical slab modes. If we retain N_* vertical slab modes in the general solution and sample each edge of $\partial\Omega_j^0$ (the boundary of Ω_j^0) by p points, then Λ_j is approximated by a $(6pN_*) \times (6pN_*)$ matrix.

The second step is to calculate the reduced DtN map $\mathcal{M}_j$ satisfying

$$\mathcal{M}_j \begin{bmatrix} \boldsymbol{w}_j \\ \boldsymbol{w}_{j-1} \end{bmatrix} = \begin{bmatrix} \mathcal{M}_{11}^{(j)} & \mathcal{M}_{12}^{(j)} \\ \mathcal{M}_{21}^{(j)} & \mathcal{M}_{22}^{(j)} \end{bmatrix} \begin{bmatrix} \boldsymbol{w}_j \\ \boldsymbol{w}_{j-1} \end{bmatrix} = \begin{bmatrix} \partial_{\boldsymbol{\nu}} \boldsymbol{w}_j \\ \partial_{\boldsymbol{\nu}} \boldsymbol{w}_{j-1} \end{bmatrix} \tag{13}$$

for electromagnetic fields satisfying the quasi-periodic condition (3), where $\boldsymbol{w}_j$ and $\boldsymbol{w}_{j-1}$ denote $\boldsymbol{w}$ on Γ_j and Γ_{j-1}, respectively. In Eq. (13), the operator $\mathcal{M}_j$ is also given in 2×2 blocks. For a regular unit cell Ω_j, its lateral boundary $\partial\Omega_j$ consists of Γ_{j-1}, Γ_j and two surfaces at $x = 0$ and $x = L$, thus Λ_j can be partitioned into 4×4 blocks accordingly. The operator $\mathcal{M}_j$ is then obtained by inserting the quasi-periodic condition (8) into Eq. (12). If Ω_j is a concave unit cell, its DtN map Λ_j is not available. However, if the lower half of Ω_j (for $0 < x < L/2$) is translated in the positive x direction by a period L, we obtain a regular unit cell with a regular hexagon cross section. Due to the quasi-periodic condition (3), $\boldsymbol{w}$ and $\partial_{\boldsymbol{\nu}}\boldsymbol{w}$ at a translated point and the original point are related by a factor of ρ. Therefore, the reduced DtN map $\mathcal{M}_j$ of a concave unit cell can be easily obtained from the reduced DtN map of a regular unit cell. Explicit formulae for this step are given in [13].

In the third step, we calculate two operators $\mathcal{Q}_m$ and $\mathcal{Q}_{m+1}$ defined on Γ_m and Γ_{m+1}. For $1 \le j \le 2m$, we define an operator $\mathcal{Q}_j$ on surface Γ_j such that

$$\mathcal{Q}_j \boldsymbol{w}_j = \partial_{\boldsymbol{\nu}} \boldsymbol{w}_j \tag{14}$$

for electromagnetic fields satisfying the Maxwell's equations (1), the quasi-periodic condition (3) and the zero boundary conditions on Γ_0 and Γ_{2m+1}. Since $\boldsymbol{w}_0 = 0$, the reduced DtN map $\mathcal{M}_1$ gives $\mathcal{Q}_1 = \mathcal{M}_{11}^{(1)}$. After that, we calculate $\mathcal{Q}_m$ by the recursion

$$\mathcal{Q}_j = \mathcal{M}_{11}^{(j)} + \mathcal{M}_{12}^{(j)} \left(\mathcal{Q}_{j-1} - \mathcal{M}_{22}^{(j)} \right)^{-1} \mathcal{M}_{21}^{(j)}, \quad j = 2, 3, \ldots, m. \tag{15}$$

The above follows directly from the definition of $\mathcal{M}_j$. A similar procedure can be used to find $\mathcal{Q}_{m+1}$ (starting from $\mathcal{Q}_{2m}$). Notice that the required number of operations for this step scales only linearly with m. Therefore, the method is capable of computing waveguide modes that decay slowly as $|y|$ is increased.

The final step is to calculate the operator $\mathcal{B}$ from the DtN map Λ_{m+1} of the central unit cell, the operators $\mathcal{Q}_m$ and $\mathcal{Q}_{m+1}$, and the quasi-periodic condition (8). We write down Λ_{m+1} in 4×4 blocks as

$$\Lambda_{m+1} \begin{bmatrix} \boldsymbol{w}_m \\ \boldsymbol{w}_{m+1} \\ \boldsymbol{w}|_{x=L} \\ \boldsymbol{w}|_{x=0} \end{bmatrix} = \begin{bmatrix} \Lambda_{11}^{(m+1)} & \Lambda_{12}^{(m+1)} & \Lambda_{13}^{(m+1)} & \Lambda_{14}^{(m+1)} \\ \Lambda_{21}^{(m+1)} & \Lambda_{22}^{(m+1)} & \Lambda_{23}^{(m+1)} & \Lambda_{24}^{(m+1)} \\ \Lambda_{31}^{(m+1)} & \Lambda_{32}^{(m+1)} & \Lambda_{33}^{(m+1)} & \Lambda_{34}^{(m+1)} \\ \Lambda_{41}^{(m+1)} & \Lambda_{42}^{(m+1)} & \Lambda_{43}^{(m+1)} & \Lambda_{44}^{(m+1)} \end{bmatrix} \begin{bmatrix} \boldsymbol{w}_m \\ \boldsymbol{w}_{m+1} \\ \boldsymbol{w}|_{x=L} \\ \boldsymbol{w}|_{x=0} \end{bmatrix} = \begin{bmatrix} \partial_{\boldsymbol{\nu}} \boldsymbol{w}_m \\ \partial_{\boldsymbol{\nu}} \boldsymbol{w}_{m+1} \\ \partial_x \boldsymbol{w}|_{x=L} \\ \partial_x \boldsymbol{w}|_{x=0} \end{bmatrix}, \tag{16}$$

where $\boldsymbol{w}|_{x=0}$ denotes $\boldsymbol{w}$ on the surface of $\partial\Omega_{m+1}$ at $x = 0$, etc. Using $\mathcal{Q}_m$ and $\mathcal{Q}_{m+1}$, we can eliminate $\boldsymbol{w}_m$, $\boldsymbol{w}_{m+1}$, $\partial_{\boldsymbol{\nu}} \boldsymbol{w}_m$ and $\partial_{\boldsymbol{\nu}} \boldsymbol{w}_{m+1}$ in Eq. (16). This leads to

$$\mathcal{U} \begin{bmatrix} \boldsymbol{w}|_{x=L} \\ \boldsymbol{w}|_{x=0} \end{bmatrix} = \begin{bmatrix} \mathcal{U}_{11} & \mathcal{U}_{12} \\ \mathcal{U}_{21} & \mathcal{U}_{22} \end{bmatrix} \begin{bmatrix} \boldsymbol{w}|_{x=L} \\ \boldsymbol{w}|_{x=0} \end{bmatrix} = \begin{bmatrix} \partial_x \boldsymbol{w}|_{x=L} \\ \partial_x \boldsymbol{w}|_{x=0} \end{bmatrix}, \tag{17}$$

where

$$\mathcal{U} = \begin{bmatrix} \Lambda_{31}^{(m+1)} & \Lambda_{32}^{(m+1)} \\ \Lambda_{41}^{(m+1)} & \Lambda_{42}^{(m+1)} \end{bmatrix} \mathcal{N} + \begin{bmatrix} \Lambda_{33}^{(m+1)} & \Lambda_{34}^{(m+1)} \\ \Lambda_{43}^{(m+1)} & \Lambda_{44}^{(m+1)} \end{bmatrix}, \tag{18}$$

$$\mathcal{N} = - \begin{bmatrix} \Lambda_{11}^{(m+1)} - \mathcal{Q}_m & \Lambda_{12}^{(m+1)} \\ \Lambda_{21}^{(m+1)} & \Lambda_{22}^{(m+1)} - \mathcal{Q}_{m+1} \end{bmatrix}^{-1} \begin{bmatrix} \Lambda_{13}^{(m+1)} & \Lambda_{14}^{(m+1)} \\ \Lambda_{23}^{(m+1)} & \Lambda_{24}^{(m+1)} \end{bmatrix}. \tag{19}$$

Using the quasi-periodic condition (8), we can further eliminate $\boldsymbol{w}|_{x=L}$ and $\partial_x \boldsymbol{w}|_{x=L}$ in Eq. (17) and obtain Eq. (10), where

$$\mathcal{B} = \mathcal{U}_{12} - \rho \mathcal{U}_{22} + \rho \mathcal{U}_{11} - \rho^2 \mathcal{U}_{21}. \tag{20}$$

If we retain N_* vertical slab modes and use p points on each edge of $\partial\Omega_j^0$, $\mathcal{M}_j$, $\mathcal{Q}_j$ and $\mathcal{B}$ are approximated by $(4pN_*) \times (4pN_*)$, $(2pN_*) \times (2pN_*)$ and $(pN_*) \times (pN_*)$ matrices, respectively. The first step (for computing Λ_j) is the most expensive, since it involves solving a linear system with a coefficient matrix of size $(6pN_*) \times (6pN_*)$. Alternatively, we can

merge the first and second steps to find the reduced DtN map $\mathcal{M}_j$ of a regular unit cell Ω_j directly. This is possible, since we can apply the quasi-periodic condition (8) to the system of equations that gives rise to Λ_j, then calculate $\mathcal{M}_j$ directly. Notice that the first step for computing Λ_j is not related to the Bloch wavenumber β. Therefore, if β is calculated for a fixed ω from Eq. (11) by an iterative method, the first step does not need to be repeated in the iterations. If ω is searched for a fixed β, then all steps must be repeated in each iteration and the alternative approach that avoids Λ_j is preferred. Typically, $\mathcal{B}$ is approximated by a matrix with a size of several hundreds, therefore, we can easily find its smallest eigenvalue $\lambda_1(\mathcal{B})$.

4. Vertical discretization

To approximate the DtN map Λ_j of a regular unit cell Ω_j, we used expansions in the eigenmodes of the slab [13]. Since the vertical directions are unbounded, the slab has a continuous spectra for the radiation and evanescent waves. To avoid the continuous spectra, we truncate the z variable to a finite interval $[d_0, d_1]$ with a stretched coordinate in two sub-intervals $[d_0, c_0]$ and $[c_1, d_1]$, where $d_0 < c_0 < 0 < c_1 < d_1$. The stretched coordinate is given by

$$\hat{z} = \int_0^z s(\tau)d\tau, \quad s(z) = \begin{cases} 1 + \sigma_0[(c_0 - z)/(c_0 - d_0)]^q, & d_0 \le z < c_0, \\ 1 + \sigma_1[(z - c_1)/(d_1 - c_1)]^q, & c_1 < z \le d_1, \\ 1, & \text{otherwise}, \end{cases} \tag{21}$$

where $q > 0$, σ_0 and σ_1 are constants. When σ_0 and σ_1 are complex, the above complex coordinate stretching corresponds to the widely used perfectly matched layer (PML) [14,15]. With this modification, the transverse electric (TE) modes of the slab satisfy

$$\frac{\mu}{s}\frac{d}{dz}\left(\frac{1}{\mu s}\frac{d\phi^{(1)}}{dz}\right) + k_0^2\varepsilon\mu\phi^{(1)} = [\eta^{(1)}]^2\phi^{(1)}, \quad d_0 < z < d_1, \tag{22}$$

$$\phi^{(1)} = 0, \quad z = d_0 \text{ and } d_1, \tag{23}$$

and the transverse magnetic (TM) modes satisfy

$$\frac{\varepsilon}{s}\frac{d}{dz}\left(\frac{1}{\varepsilon s}\frac{d\phi^{(2)}}{dz}\right) + k_0^2\varepsilon\mu\phi^{(2)} = [\eta^{(2)}]^2\phi^{(2)}, \quad d_0 < z < d_1, \tag{24}$$

$$\frac{d\phi^{(2)}}{dz} = 0, \quad z = d_0 \text{ and } d_1. \tag{25}$$

The PML technique is very effective for modeling outgoing radiation waves and it is needed to calculate out-of-plane radiation loss for scattering problems in PhC slabs [13]. On the other hand, the electromagnetic fields of a guided mode of a PhC slab waveguide decay exponentially as $z \to \pm\infty$, thus a PML is really not needed. However, it is still beneficial to

take real and positive values for σ_0 and σ_1. Such a real coordinate stretching gives a large effective truncation interval for z. It produces the effect of a non-uniform mesh when a simple uniform mesh in z is used.

In [13], we developed a compact fourth order finite difference scheme to discretize Eqs. (22) and (24). A staggered grid is used for z, such that the TE and TM modes are calculated on the integer and half-integer grid points, respectively. If the grid size is $\Delta z = (d_1 - d_0)/N$ for a positive integer N, then the numerical scheme gives $N - 1$ TE modes and N TM modes. Thus, the total number of numerical eigenmodes is $N_* = 2N - 1$.

5. Numerical examples

To illustrate our method, we consider a waveguide previously analyzed by a number of authors [5]. The PhC slab is a triangular lattice of air holes with radius $0.29L$, where L is the lattice constant. The thickness and the dielectric constant of the slab are $0.6L$ and $\varepsilon = 11.56$ respectively, and it is surrounded by air. The PhC slab has a bandgap for normalized frequency $\omega L/(2\pi c)$ from 0.256 to 0.32. The waveguide is formed by filling a row of air holes as shown in Fig. 1. In our calculations, the z variable is truncated to the interval $[d_0, d_1]$ with $d_1 = -d_0 = 1.5L$. The coordinate is stretched in the intervals $[d_0, c_0]$ and $[c_1, d_1]$, where $c_1 = -c_0 = 0.9L$. Other parameters in the stretching function (21) are $\sigma_0 = \sigma_1 = 10$ and $q = 3$. For truncating the y direction, we use $m = 10$, so that the truncated domain S_m contains 21 unit cells. For $N = 80$ and $p = 7$, the vertical grid size is $\Delta z = 0.0375L$, the total number of vertical slab modes is $N_* = 159$, the operators Λ_j, $\mathcal{M}_j$, $\mathcal{Q}_j$ and $\mathcal{B}$ are approximated by matrices of size 6678×6678, 4452×4452, 2226×2226 and 1113×1113, respectively. Our numerical results are are shown in Fig. 3, and they are consistent with previous calculations. The top panel of Fig. 3 shows the calculated Bloch wavenumbers for given frequencies. Since parts of the dispersion curves are very flat, it is necessary to use small increments in ω to obtain the complete curves. Since a small change in the frequency may give rise to a large change in β, the method may take more than 20 iterations to convergent, even when a previously calculated β for a nearby frequency is used as the initial guess. In Fig. 3 (lower panel), we show the numerical results obtained by solving ω for a fixed β. In that case, the alternative approach that calculates $\mathcal{M}_j$ directly (without Λ_j) is used. On a computer with an Intel Xeon 2.33GHz CPU, one iteration requires about three minutes. If a previously calculated ω for a nearby β is used as the initial guess, the method requires only 3 or 4 iterations to find a converged solution of ω.

To gain a better understanding of our method, we carry out some convergence tests. Although the coordinate stretching parameters σ_0 and σ_1 can be optimized using the procedure developed in [16], we fix $\sigma_0 = \sigma_1 = 10$ in the following calculations for simplicity. In the first test, we fix the frequency at $\omega L/(2\pi c) = 0.264$ and keep the number of points on each edge

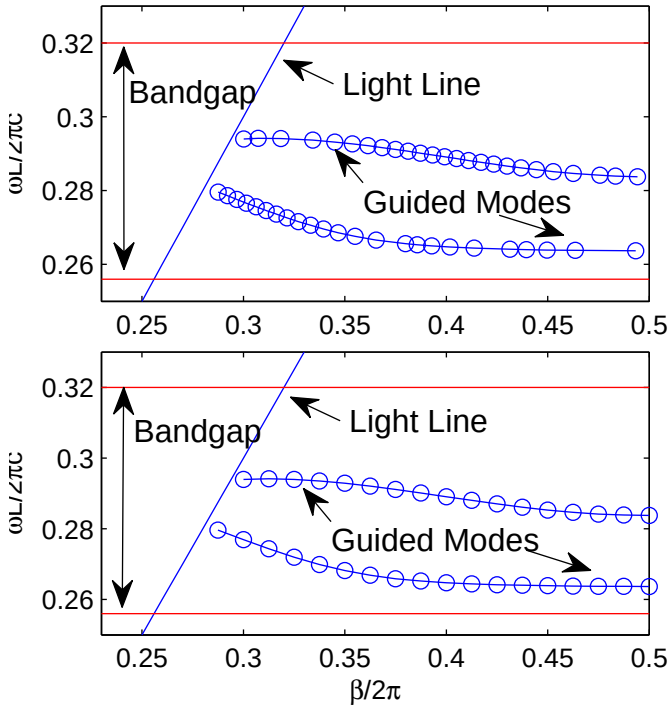

Fig. 3. Dispersion relations of the guided modes of a PhC slab waveguide calculated by solving the nonlinear equation (11) for given frequencies (top) or given Bloch wavenumbers (bottom).

of $\partial\Omega_j^0$ at $p = 7$, then compare the numerical results obtained using different number of points in the vertical direction. The results are shown in Table 1. The first column lists the integer N which is related to the grid size by $\Delta z = (d_1 - d_0)/N$ and the total number of slab modes by $N_* = 2N - 1$. The second and third columns of Table 1 list the relative errors of the numerical solutions for $\eta_1^{(1)}$ and $\eta_1^{(2)}$, which are the propagation constants of the first TE and TM slab modes. The last column gives the normalized propagation constant of a guided mode of the PhC slab waveguide. From the results in Table 1, it appears that three correct digits can be obtained with $N \geq 80$. In the second test, we fix $N = 80$ and compare the numerical results for different values of p. With the other parameters remain the same, we obtain the results in Table 2. Consistent with our previous experience for 2D PhCs, the odd integers p tend to give more accurate solutions. It appears that 4 correct digits can be obtained if $p \geq 7$.

Table 1. Numerical convergence of vertical slab modes and a PhC slab waveguide mode with respect to the number of points for discretizing the vertical direction.

N	R.E. for $\eta^{(1)}$	R.E. for $\eta^{(2)}$	$\beta L/2\pi$
20	1.1×10^{-4}	1.1×10^{-3}	0.4414
30	1.4×10^{-5}	2.3×10^{-4}	0.4404
40	3.6×10^{-6}	7.3×10^{-5}	0.4396
50	1.3×10^{-6}	3.0×10^{-5}	0.4391
60	6.0×10^{-7}	1.5×10^{-5}	0.4388
80	1.8×10^{-7}	4.8×10^{-6}	0.4384
100	6.9×10^{-8}	2.1×10^{-6}	0.4382
120	3.3×10^{-8}	1.2×10^{-6}	0.4381
140	1.7×10^{-8}	7.4×10^{-7}	0.4381
160	1.0×10^{-8}	5.4×10^{-7}	0.4380
180	6.2×10^{-9}	4.3×10^{-7}	0.4380

6. Conclusions

In this paper, we developed an efficient numerical method for computing guided modes of photonic crystal slab waveguides. The method formulates a nonlinear eigenvalue problem on a small surface in the waveguide core. Compared with standard numerical methods discretizing the three-dimensional domain for one period of the waveguide, matrices in our method are much smaller. Although the problem is nonlinear, it can be efficiently solved by simple iterative methods, such as the secant method. Our method relies on the Dirichlet-to-Neumann (DtN) maps of the unit cells constructed in a previous work [13] to avoid repeated calculations in identical unit cells. The DtN map of a unit cell maps the z components of the electromagnetic fields to their normal derivatives on the lateral boundary of the unit cell. Since the DtN maps are constructed using expansions in vertical slab modes and horizontal cylindrical waves, a discretization in the horizontal plane is avoided. Our method is capable of computing waveguide modes that decay slowly away from the core in the horizontal plane. Although the resolution in the vertical direction sets a limit on the accuracy of the numerical solutions, three or four digits can be easily obtained with relatively little computing effort. The present work is only concerned with true guided modes for PhC slab waveguides. If the vertical variable z is properly truncated by PMLs, the method may be used to calculate leaky modes for PhC slab waveguides with out-of-plane losses.

Table 2. Numerical convergence of a PhC slab waveguide mode with respect to the number of sampling points on each edge of the hexagon cross section of regular unit cells.

p	$\beta L/2\pi$
3	0.438955
4	0.436168
5	0.438323
6	0.438543
7	0.438422
8	0.438409
9	0.438415

Acknowledgments

This research was partially supported by a grant from City University of Hong Kong (Project No. 7008054).

References

1. J. D. Joannopoulos, S. G. Johnson, J. N. Winn, and R. D. Meade, Photonic Crystals: Molding the Flow of Light, 2nd Ed. (Princeton University Press, Princeton, NJ, 2008).
2. T. Baba, N. Fukaya, and Y. Yonekura, "Observation of light propagation in photonic crystal optical waveguides with bends," Electron. Lett. **35**, 654-655 (1999).
3. S. Y. Lin, E. Chow, S. G. Johnson, and J. D. Joannopoulos, "Demonstration of highly efficient waveguiding in a photonic crystal slab at the 1.5μm wavelength," Opt. Lett. **25**, 1297-1299 (2000).
4. M. Loncar, D. Nedeljkovic, T. Doll, J. Vuckovic, A. Scherer, and T. P. Pearsall, "Waveguiding in planar photonic crystals," Appl. Phys. Lett. **77**, 1937-1939 (2000).
5. A. Chutinan and S. Noda, "Waveguides and waveguide bends in two-dimensional photonic crystal slabs," Phys. Rev. B **62**, 4488-4492 (2000).
6. S. G. Johnson, P. R. Villeneuve, S. Fan, and J. D. Joannopoulos, "Linear waveguides in photonic-crystal slabs," Phys. Rev. B **62**, 8212-8222 (2000).
7. G. R. Hadley, "Out-of-plane losses of line-defect photonic crystal waveguides," IEEE Photon. Technol. Lett. **14**, 642-644 (2002).
8. P. Lalanne, "Electromagnetic analysis of photonic crystal waveguides operating above the light core," IEEE J. Quantum Electron. **38**, 800-804 (2002). IEEE J. Quantum

Electron.

9. C. Sauvan, P. Lalanne, J. Rodier, J. Hugonin, and A. Talneau, "Accurate modeling of line-defect photonic crystal waveguides," IEEE Photon. Technol. Lett. **15**, 1243-1245 (2003).
10. Y. Huang, Y. Y. Lu, and S. Li, "Analyzing photonic crystal waveguides by Dirichlet-to-Neumann maps," J. Opt. Soc. Am. B **24**, 2860-2867 (2007).
11. S. Li and Y. Y. Lu, "Efficient method for computing leaky modes in two-dimensional photonic crystal waveguides," J. Lightwave Technol. **28**, 978-983 (2010).
12. Y. Huang and Y. Y. Lu, "Scattering from periodic arrays of cylinders by Dirichlet-to-Neumann maps," J. Lightwave Technol. **24**, 3448-3453 (2006).
13. L. Yuan and Y. Y. Lu, "Dirichlet-to-Neumann map method for analyzing hole arrays in a slab," J. Opt. Soc. Am. B **27**, 2568-2579 (2010).
14. J. Berenger, "A perfectly matched layer for the absorption of electromagnetic waves," J. Comput. Phys. **114**, 185-200 (1994).
15. W. C. Chew and W. H. Weedon, "A 3-D perfectly matched medium from modified maxwell's equations with stretching coordinates," Micro. Opt. Tech. Lett. **7**, 599-604 (1994).
16. Y. Y. Lu, "Minimizing the discrete reflectivity of perfectly matched layers," IEEE Photon. Technol. Lett. **18**, 487-489 (2006).